www.ietdl.org

Published in IET Intelligent Transport Systems
Received on 13th December 2011
Revised on 11th September 2012
Accepted on 3rd October 2012
doi: 10.1049/iet-its.2011.0224

ISSN 1751-956X

# Modelling correlation degree between two adjacent signalised intersections for dynamic subarea partition

*Yiming Bie[1], Dianhai Wang[2], Xiaobo Qu[3]*

*[1]School of Transportation Science and Engineering, Harbin Institute of Technology, Harbin, Heilongjiang 150091, People's Republic of China*
*[2]Department of Civil Engineering and Architecture, Zijingang Campus, Zhejiang University, Hangzhou 310058, People's Republic of China*
*[3]Griffith School of Engineering, Gold Coast campus, Griffith University, QLD 4222, Australia*
*E-mail: yimingbie@126.com*

**Abstract:** Correlation degree between adjacent signalised intersections is considered as the most important component in subarea partition algorithm. In this study, contributing factors for subarea partition are selected by taking into consideration the differences with respect to cycle lengths, link length and path flow between upstream and downstream coordinated phases. Their impacts on performance index of subarea partition are further studied using numerical experiments. The study then proceeds to propose a correlation degree index (CI) as an alternative for the performance index in order to reduce the computational complexity. The relationship between CI and the contributing factors is established to predict the correlation degree. Finally, the model is validated using field survey data.

## 1 Introduction

Subarea partition is of great importance to traffic control system since the selection of signal timing method for each intersection is determined by the partition results. Within a given subarea, the cycle lengths and phasing plans for different intersections are designed in such a way as to facilitate progressive movements and thereby reduce number of stops and delay [1].

The objective of subarea partition is to identify whether control performance can be improved when signal coordinated mode is implemented to adjacent intersections. If the performance is improved, the adjacent intersections can be partitioned into one subarea. Therefore a straightforward method for subarea partition is to calculate and compare the control performances with respect to signal coordinated mode and isolated control mode. However, this method is not easy to be implemented in practice, although it is uncomplicated. This is because it would be time consuming to iteratively estimate the performances of hundreds of adjacent intersections. Thus, an effective alternative is to propose an index reflecting the changes of control performances indirectly, which is called correlation degree index (CI) in this paper. As an appropriate alternative to control performances with a simpler form, it should accurately predict the change of control performances. Accordingly, the development of a model for CI is of great significance to subarea partition.

However, from the literature, little has been done on subarea partition, although it is essential in reality. The concept of subarea partition was first raised by Walinchus [2]. In his study, the contributing factors of subarea partition included the locations of significant changes in traffic flow characteristics (e.g. freeway access points from service roads, major arterials changed into urban grids etc.). His study provided the fundamental basis for further study in subarea partition. Yagoda [3] concluded that the degree of coupling requirement was directly proportional to traffic volume ($V$) and inversely proportional to link length ($L$) between two adjacent intersections. Thus, a coupling index ($I$) was defined as $I = V/L$. Greater index indicates more desirable to have the two intersections coupled. Although the model is theoretically sound, it lacks of reflecting the complex changes in traffic pattern between two adjacent intersections. Chang [4] brought in the concept of interconnection desirability index by considering both flow pattern and platoon dispersion characteristic. If the value of the index was greater than 0.35, two intersections should be grouped. Bie *et al.* [5] demonstrated that the index could not vary quickly as the traffic state change. Lin and Tsao [1] selected congestion index of intersection, critical block length, and continuation of traffic movement as factors that may affect the performance of subarea partition. Mathematical equations were established to quantify these factors. However, the authors did not establish the relationship between control performance and the contributing factors. Lin and Huang [6] developed a linear model for determining coordination of two adjacent signalised intersections from the view of block length. The model consisted of the dependent variable critical block length, and the independent variables original platoon size and platoon completeness ratio. A deficiency of the study is that block length itself only depicts partial picture of factors that affects subarea partition. Bie *et al.* [5] chose not only cycle length but also platoon length as contributing factors. An integrated correlation model was developed to quantify the correlation degree between two adjacent intersections. However, the determinations of weighted coefficients in the model and threshold value were dependent on experiences and lack of theoretical basis. Synchro [7] is perhaps the only software that has a feature of subarea partition application. The software calculates an empirical coordinatability factor based on several variables such as distance, travel time and traffic volume. The coordinatability factor provides indications whether an intersection should be coordinated with other signals in the system. For example, a coordinatability factor of 100 means the signal should be coordinated with other signals, whereas a factor below 20 would suggest that the signal operates better independently. Tian and Urbanik [8] proposed a heuristic approach that divided a large signalised arterial into subsystems with three to five signals in each subsystem. Each subsystem was optimised to achieve the maximum bandwidth efficiency.

Even in modern traffic adaptive control systems, studies pertaining to correlation model and subarea partition are also not many. In split, cycle and offset optimisation technique (SCOOT) [9], the network was partitioned on the basis of experiences of engineers and the form of subarea was fixed with traffic demand variation. In Sydney coordinated adaptive traffic system (SCATS), a simple index of integration or disjunction of subareas was proposed based on the differences between cycle lengths [10]. In real time hierarchical optimised distributed effective system (RHODES), it was expected that nine intersections could be controlled as the reasonable size of a subarea without enormous computational effort [11].

As for real-time traffic control systems, an appropriate CI should reflect dynamic characters of traffic flow and interactions among adjacent intersections. The objective of this study is to propose an approach that is able to estimate a dynamic CI between two adjacent intersections for subareas partition. Contributing factors are taken into account in the proposed correlation degree model. This study could be the groundwork for CI among multiple intersections.

## 2 Development of correlation degree model

### 2.1 Contributing factors of correlation degree

The factors that affect the improvement of signal coordination would also be those affect subarea partition. In this section, the factors that should be included in subarea partition are described. These factors are the difference of cycle lengths between two adjacent intersections, link length and path flow between upstream and downstream coordinated phases.

*2.1.1 Difference of cycle lengths between two adjacent intersections:* Intersections in a subarea usually execute common cycle length (CCL) as to obtain maximum green wave bandwidth and maintain optimal offsets. For a subarea with two intersections, the intersection that operates maximum cycle length (MCL) is determined as seed intersection and its cycle length is set as CCL. However, vehicle delay of the other intersection would increase because CCL may be larger than its optimal cycle length (OCL). The increase range is directly proportional to the difference between CCL and OCL. When the difference is large enough, the increased vehicle delay may be larger than the delay reduced by signal coordination.

*2.1.2 Link length between two adjacent intersections:* Signal coordination can reduce vehicle delay by providing green time for coming traffic platoon. A compact platoon proves to be effective in improving coordination benefits because more vehicles may pass the stop line in green time. According to Robertson's platoon dispersion model [12], original platoon departs from upstream stop line would disperse to some extent and the dispersion level is directly proportional to link length. Accordingly, a long link would have a negative impact on arterial progression.

*2.1.3 Path flow between upstream and downstream coordinated phases:* When a platoon that departs from upstream coordinated phase travels to downstream intersection, some vehicles in the platoon may turn to uncoordinated downstream phases. Therefore the path flow that between the upstream and downstream coordinated phases may be less than the original flow departs from upstream coordinated phase. Larger path flow indicates more vehicles travel between the two phases and more vehicle delays have the opportunity to be reduced by signal coordination. Thus, the correlation degree is directly proportional to the path flow.

### 2.2 Performance index

The performance index of subarea partition should change as the traffic states of intersections vary. For example, the purpose of partitioning unsaturated adjacent intersections is to reduce vehicle delay. However, for saturated adjacent intersections, the purpose is to maximise capacity or minimise queue length. In this paper, we only study the unsaturated adjacent intersections, thus vehicle delay is selected as the performance index.

Let us take two adjacent intersection $i$ and $j$ for example. Their total vehicle delay per cycle is denoted as $D_i$ and $D_j$ when running isolated control mode. $D_i$ or $D_j$ can be obtained by the delay function in HCM 2000 [13]. If the two intersections are grouped into one subarea, they would run signal coordinated mode. In such situation, total vehicle delay per cycle is denoted as $\widehat{D}_i$ and $\widehat{D}_j$. The improved performance of grouping $i$ and $j$ into one subarea can be obtained by the following equation

$$\begin{aligned} \mathrm{PI} &= D - \widehat{D} \\ &= \left(D_i \frac{3600}{C_i} + D_j \frac{3600}{C_j}\right) - (\widehat{D}_i + \widehat{D}_j)\frac{3600}{\max(C_i, C_j)} \end{aligned} \quad (1)$$

In (1), $C_i$ is the OCL of $i$ when running isolated control mode, $\max(C_i, C_j)$ is the CCL when running signal coordinated mode, $D$ is the total vehicle delay per hour with respect to isolated control mode and $\widehat{D}$ is the total vehicle delay per hour with respect to signal coordinated mode. All evaluation indices are unified as total vehicle delay per hour (the unit of PI is s/h). Because the OCL of non-seed intersection may be smaller than the CCL. Thus, the number of arrival vehicles each cycle may also be smaller than that when operating different timing modes.

PI is larger than 0 indicates that signal coordinated mode can obtain better performance than isolated control mode, therefore intersection $i$ and $j$ can be partitioned into one subarea. Otherwise $i$ and $j$ must be partitioned into different subareas.

### 2.3 Quantification the impact of difference of cycle lengths on CI

The best way to analyse the impact of difference of cycle lengths on PI is to develop a function between them based on theoretical derivation, and then calculate the variable quantity of PI resulting from the unit change in difference of cycle lengths. However, $D$ in (1) is difficult to be obtained because of complex characters of vehicle movements on consecutive intersections. Thus, numerical experiments are adopted in this paper.

Also taking intersection $i$ and $j$, for example link length $L$ equals 400 m and average vehicle speed is 12 m/s. $j$ is the seed intersection and $i$ is the non-seed intersection. When the intersections run signal coordination, the OCL of $j$ is set as the CCL. The difference between OCL of $i$ and CCL increases with a step of 5 s whereas link length and path flow are fixed. Table 1 shows the output results of two experimental scenarios. In the two scenarios, CCL equals 125 and 110 s, respectively. In Table 1, the improved range equals the proportion of PI to $D$. The larger the range is, the better the signal coordination benefits are.

Take scenario 1 as an example, when OCL of $i$ equals 90 s, the difference between cycle lengths is 35 s and PI equals 20 044 s. The improved range is only 5.7%. However, when OCL of $i$ increases to 125 s, the improved range is 17.24%. The difference is negatively correlated to the improved range and the similar trend is obtainable in other scenarios. The results indicate that the difference between cycle lengths has a substantial impact on PI.

The data shown in Table 1 can also be interpreted as follows. When the difference equals 0, signal coordination can obtain maximum benefits, which means the correlation between the two intersections is maximal and CI is 1.0. However, when the difference equals 35 s, the proportion of the improved range out of that when the difference equals 0 is only 33%, that is CI decreases to 0.33.

**Table 1** Output results of the two experimental scenarios

| Scenario | OCL of *i*,s | OCL of *j*, s | *D* , s/h | PI, s/h | Improved range, % |
|---|---|---|---|---|---|
| 1 | 90 | 125 | 351 576 | 20 044 | 5.70 |
| | 95 | | 358 915 | 25 438 | 7.09 |
| | 100 | | 371 277 | 34 919 | 9.41 |
| | 105 | | 378 642 | 40 453 | 10.68 |
| | 110 | | 390 619 | 50 311 | 12.88 |
| | 115 | | 399 471 | 57 848 | 14.48 |
| | 120 | | 408 876 | 65 726 | 16.07 |
| | 125 | | 416 925 | 71 878 | 17.24 |
| 2 | 90 | 110 | 322 504 | 22 407 | 6.95 |
| | 95 | | 331 007 | 28 399 | 8.58 |
| | 100 | | 342 658 | 37 425 | 10.92 |
| | 105 | | 351 739 | 44 573 | 12.67 |
| | 110 | | 360 691 | 51 658 | 14.32 |

As can be seen from Table 1, CI is affected by not only the difference of cycle lengths, but also the CCL. Thus, the difference of cycle lengths is normalised as follows.

$$C_{\mathrm{D}} = \frac{C_j - C_i}{C_j} \tag{2}$$

For the two scenarios, the scatter diagrams between CI and normalised difference of cycle lengths $C_{\mathrm{D}}$ are shown in Fig. 1.

There is a strong linear relationship between CI and $C_{\mathrm{D}}$, and a linear function can be used to fit their relationship. The fitting formulas for the two subfigures are shown as follows

$$\mathrm{CI} = \begin{cases} -2.471C_{\mathrm{D}} + 1.024, & R^2 = 0.995 \\ -2.894C_{\mathrm{D}} + 1.009, & R^2 = 0.996 \end{cases} \tag{3}$$

Linear functions can fit the scatter diagrams very well as indicated by the high $R^2$ values. However, problem is that the slopes of the two lines are different from each other. This indicates that in different scenarios, $C_{\mathrm{D}}$ would pay different impacts on CI. Therefore a universal function is needed to depict the relationship between the two variables, and to make the slope vary as traffic state changes. The linear functions in (3) can be replaced by the following format

$$\mathrm{CI}(C_{\mathrm{D}}) = \alpha_1 C_{\mathrm{D}} + b_1 \tag{4}$$

where $\alpha_1$ is the slope of the function, and $b_1$ is the intercept.

In reality, $b_1$ should equal 1.0. However, because of fitting errors of (3), there exist marginal differences between the intercepts and 1.0. In this study, the differences are neglected and the value of $b_1$ is set as 1.0 directly. Therefore only $\alpha_1$ is needed to be fit in (4). $\alpha_1$ represents the variable quantity of CI resulting from the unit change in $C_{\mathrm{D}}$. It may be affected by many factors, such as green split and volume-to-capacity ratio ($v/c$) of coordinated phases, $v/c$ of uncoordinated phases, total $v/c$, CCL and intersection saturation degree $x$. To study the impacts of these factors on $\alpha_1$, a multivariate regression can be adopted. The factors are introduced into the fitting function firstly and then eliminating the variables stepwise according to the correlation until the given precision is achieved. Then residual variables in the function are those pay significant impacts on $\alpha_1$. The amount of data in Table 1 is not enough for the regression model. Accordingly, another six experiments are carried out and total eight groups of data are obtainable. The regression function is shown in the following equation

$$\alpha_1 = 14.916 - 53.963x + 4.831\lambda_{\mathrm{c}} + 36.281Y, \quad R^2 = 0.92 \tag{5}$$

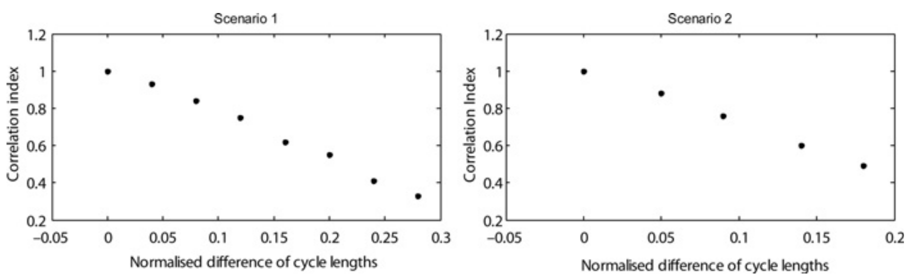


**Fig. 1** *Scatter diagrams between CI and normalised difference of cycle lengths*



doi: 10.1049/iet-its.2011.0224

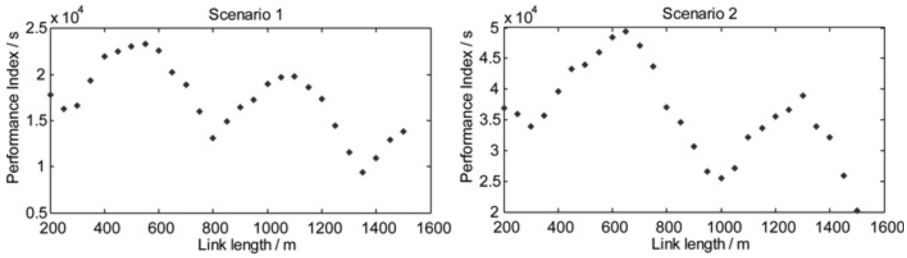


**Fig. 2** *Scatter diagrams between L and PI of the two scenarios*

In the function, $\lambda_c$ is the green split of coordinated phase and $Y$ is total *v/c*. Only three variables are left and other variables are excluded. $F$-test is carried out to identify whether the real value and fitted value of $\alpha_1$ differ significantly under a given significance level of 0.05, and the results of the test is acceptable.

### 2.4 Quantification the impact of link length on CI

Numerical experiments are conducted to establish the relationship between link length $L$ and CI. During the experiments, $L$ is increased from 200 m to 1500 m with a step of 50 m whereas cycle lengths of the two intersections and the path flow between coordinated phases are fixed in each scenario. Besides, cycle lengths of intersection $i$ and $j$ are same to each other. Fig. 2 shows the output results of two typical scenarios. In scenario 1 and 2, the cycle lengths of $i$ and $j$ equal 90 s.

In Fig. 2, $L$ and PI have a curvilinear relationship and the two curve shapes are similar to each other. As the value of $L$ increases, the value of PI increases up to a maximum, which is attained at $L$ equals about $0.5C_jV$. As $L$ increases further, PI decreases and reaches a minimum value at $L$ equals about $0.75C_jV$. The cycle is repeated along the increase of $L$ with a step size of $0.5C_jV$ m. Difference is that the values of maximum and minimum decrease step by step. This changing tendency is significantly different with our straightforward view, because traditionally we think PI would decrease linearly with the increase of $L$. However, the straightforward view is based on one-directional signal coordination and in this study we mainly focus on dual-directional signal coordination of the two adjacent intersections. When $L$ equals the integral multiple of $0.5C_jV$, dual-directional interactive coordination is the best and thus traffic control can obtain maximum benefits. When $L$ equals odd times of $0.25C_jV$, dual-directional coordination produces worst benefits and thus PI is minimal.

In numerical experiments $L$ is increased with a step of 50 m and the integer times of $0.25C_jV$ do not equal the integer times of 50. Thus, to obtain the exact curvilinear relationship between $L$ and PI, the values of PI corresponding to integer times of $0.25C_jV$ are supplemented.

When PI reach maximum value at $L$ equals $0.5C_jV$, partition the two intersections into one subarea can obtain maximum control benefits, in such case CI equals 1.0. In other cases, CI equals the proportion of PI out of the maximum value of PI. $L$ is normalised as follows

$$L_c = \frac{L}{L_{max}} \tag{6}$$

where $L_c$ is the normalised link length. $L_{max}$ is recommended as 1500 m in this study because signal coordination is not suitable when $L$ is larger than 1500 m according to engineering experiences. The relationship between CI and $L_c$ is similar to that in Fig. 2. Thus, the scatter diagrams between them are not displayed.

It is found that piecewise linear function may be suitable to fit the curve after detailed analysis. Moreover, the differences of two adjacent minimal values of CI are nearly a constant, and the differences between maximal values of CI and its left minimal values are also nearly a constant. For scenarios 1 and 2, the extreme values of CI corresponding to integer times of $0.25C_jV$ are shown in Table 2.

In scenario 1, the difference between the first maximum and minimum equals 0.337. The difference between the second maximum and minimum equals 0.325. The two numbers are very close. Besides, the difference between the first minimum and second minimum equals 0.130. The difference between the second minimum and third minimum equals 0.133. They are also very close. In scenario 2 the same phenomenon is obtainable. The extreme points of the $L_c$–CI curve are labelled and shown in Fig. 3 to model conveniently.

In numerical experiments, $L$ ranges from 200 to 1500. However, $L$ should be larger than 0. Thus, in Fig. 3 the section that $L$ belongs to the interval [0, 200] is supplemented to make the curve intact. But the values of CI corresponding to that interval do not have practical meanings. Because when $L$ is smaller than 200 m, the objective of signal control should be to minimise queue length or avoid queue spillovers, other than reduce vehicle delay. On the basis of the changing tendency of CI, $y$ (0) should be larger than 1.0. But it does not have practical meaning. Therefore it is set as 1.0 to model conveniently.

To fit the curve in Fig. 3 using piecewise linear function, the values of $y(1)$ and $y(3)$ are needed. The difference between $y(2)$ and $y(1)$ represents the reduction range of CI when the link length decreases from $0.5C_jV$ to $0.25C_jV$. Similarly, the difference between $y(2)$ and $y(3)$ represents the reduction range of CI when the link length increases from $0.5C_jV$ to $0.75C_jV$. The reduction ranges are affected

**Table 2** Values of CI corresponding to the extreme points

| Scenario | First minimum | First maximum | Second minimum | Second maximum | Third minimum |
|---|---|---|---|---|---|
| 1 | 0.663 | 1 | 0.533 | 0.858 | 0.4 |
| 2 | 0.674 | 1 | 0.527 | 0.816 | 0.372 |

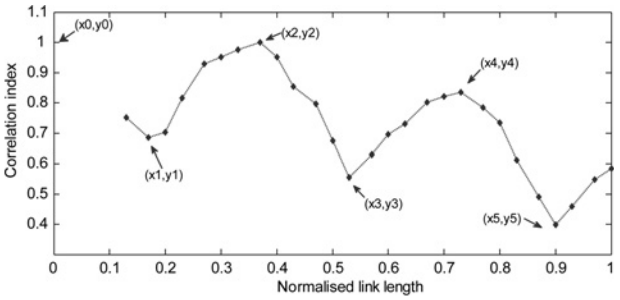


**Fig. 3** *Scatter diagram between $L_c$ and CI in scenario 1*

by many factors, such as CCL, green split and *v/c* of coordinated phase, *v/c* of uncoordinated phases, total *v/c* and saturation degree *x*. The multivariate regression method shown in Section 2.3 is also adopted here to distinguish whether the above factors pay significant impacts on $y(1)$ and $y(3)$. Total ten groups of data are used in the regression.

The regression functions are shown in (7). In the two functions, only $x$, $y_c$ and $Y$ are left and other variables are excluded. $y_c$ is the *v/c* ratio of coordinated phase

$$\begin{cases} y(1) = 0.381 + 0.992x - 0.87Y + 0.291y_c, & R^2 = 0.95 \\ y(3) = -2.716 + 11.682x - 9.814Y + 1.942y_c, & R^2 = 0.96 \end{cases} \tag{7}$$

Then $y(n)$ in the $L_c$–CI curve equals

The $n$th one in the sets of lines can be fitted by the following equation

$$\mathrm{CI}_n(L_c) = \alpha_2 L_c + b_2$$
$$\begin{cases} \alpha_2 = \dfrac{y_n - y_{n-1}}{x_n - x_{n-1}} \\ b_2 = \left( y_{n-1} - \dfrac{y_n - y_{n-1}}{x_n - x_{n-1}} x_{n-1} \right) \end{cases} \tag{9}$$

where $\alpha_2$ is the slope of the line, and $b_2$ is the intercept.

For scenario 1, the function between $L_c$ and CI equals

$$\mathrm{CI}(L_c) = \begin{cases} -1.872L_c + 1.0, & 0 \le L_c \le 0.18 \\ 1.872L_c + 0.326, & 0.18 < L_c \le 0.36 \\ -2.594L_c + 1.934, & 0.36 < L_c \le 0.54 \\ 1.871L_c - 0.478, & 0.52 < L_c \le 0.72 \\ -2.595L_c + 2.738, & 0.72 < L_c \le 0.90 \\ 1.871L_c - 1.282, & 0.90 < L_c \le 1.0 \end{cases} \tag{10}$$

The results of $F$-test show that there is no significant difference between the real values and fitted values of CI. Thus, (10) can be used to depict the relationship between $L_c$ and CI in scenario 1.

### 2.5 Quantification the impact of path flow on CI

Let $q_s$ denotes the path flow and the maximum value of $q_s$ (denoted as $q_{s\max}$) equals the maximum arrival flow of upstream coordinated phase. Because signal coordination is not suitable to be implemented to the intersection of which saturation degree is larger than $X$, thus $q_{s\max}$ is determined as the maximum historical traffic volume of upstream coordinated phase when its saturation degree is not larger than $X$. In this study, $X$ is recommended as 0.90, because traffic jam may occur to one intersection when its saturation degree is larger than 0.90.

Also take intersection $i$ and $j$ for example. Two scenarios are tested firstly. Intersection $i$ and $j$ have the same cycle length and saturation degree. $q_{s\max}$ of the two scenarios are 640 and 670 pcu/h, respectively. The two-directional path flows are the same. $q_s$ is decreased from $q_{s\max}$ with a step of 5% $q_{s\max}$ whereas cycle length and link length are fixed.

Table 3 shows the output results. In the table $P_q$ is the proportion of the difference between $q_s$ and $q_{s\max}$ to $q_{s\max}$, which increases from 0 to 40%. $D_u$ is the total vehicle delay per hour of uncoordinated phases. To keep the cycle length be fixed in each scenario, the reduced path flow is added to uncoordinated phases equally. Thus, the traffic flow and vehicle delay of uncoordinated phases would increase. $D_c$ is the total vehicle delay per hour of coordinated phase. Because traffic volume of coordinated phase decreases gradually, $D_c$ also decreases. $P_{dc}$ is the decreased vehicle delay of coordinated phase compared with that when $P_q$ equals 0. $P_{du}$ is the increased vehicle delay of uncoordinated phases compared with that when $P_q$ equals 0. $\mathrm{PI}_n$ is the negative performance index resulted by the decrease of $q_s$. $P_n$ is the proportion of $\mathrm{PI}_n$ to the PI when $P_q$ equals 0.

In Table 3, the signal control between the two intersections can obtain maximum benefits when $P_q$ equals 0. Therefore CI equals 1.0. $P_n$ indicates the degradation of PI with the increase of $P_q$. Take scenario 1 for example, $P_n$ is 14.99% when $P_q$ equals 15%. In such case the control benefits equal 85.01% of the PI when $P_q$ equals 0. That is, CI equals 0.8501. CI is the difference between 1.0 and $P_n$. $P_q$ can be used as the normalised index of path flow. The scatter diagram between $P_q$ and CI of the two scenarios are shown in Fig. 4.

As can be seen from Fig. 4, there is a strong linear relationship between $P_q$ and CI. Linear function can be used to fit the scatter diagrams. The fitted functions are shown in (11). $R^2$ of the two functions are all larger than 0.94, which indicate that linear function can fit the relationship well

$$\begin{cases} \mathrm{CI}(P_q) = -0.828P_q + 0.9973, & R^2 = 0.95 \\ \mathrm{CI}(P_q) = -0.401P_q + 0.9726, & R^2 = 0.94 \end{cases} \tag{11}$$

Problem is that the slopes of the two functions are different. The slope is affected by many factors, such as CCL, green split and *v/c* of coordinated phase, *v/c* of uncoordinated

$$y(n) = \begin{cases} 1.0 & n = 0 \\ 0.381 + 0.992x - 0.87Y + 0.291y_c & n = 1 \\ 1.0 & n = 2 \\ -2.716 + 11.682x - 9.814Y + 1.942y_c & n = 3 \\ y(n-1) + y(n-2) - y(n-3) & n \ge 4 \text{ and even integer} \\ y(n-2) + y(n-4) - y(n-2) & n \ge 4 \text{ and odd integer} \end{cases} \tag{8}$$



doi: 10.1049/iet-its.2011.0224

**Table 3** Impact of difference between $q_s$ and $q_{smax}$ on control benefits

| Scenario | $P_q$, % | $D_u$, s | $D_c$, s | $P_{dc}$, s | $P_{du}$, s | $PI_n$ | $P_n$, % |
|---|---|---|---|---|---|---|---|
| 1 | 0 | 265 103 | 77 701 | 0 | 0 | 0 | 0.00 |
| | 5 | 271 860 | 72 611 | 5090 | 6757 | 1667 | 3.08 |
| | 10 | 276 639 | 69 391 | 8310 | 11 536 | 3226 | 5.95 |
| | 15 | 283 045 | 67 884 | 9817 | 17 942 | 8124 | 14.99 |
| | 20 | 287 528 | 64 228 | 13 473 | 22 425 | 8951 | 16.52 |
| | 25 | 297 323 | 59 695 | 18 006 | 32 220 | 14 214 | 26.23 |
| | 30 | 299 637 | 57 025 | 20 676 | 34 534 | 13 858 | 25.57 |
| | 35 | 305 460 | 53 310 | 24 391 | 40 357 | 15 965 | 29.46 |
| | 40 | 309 357 | 49 541 | 28 160 | 44 254 | 16 094 | 29.69 |
| 2 | 0 | 198 840 | 59 700 | 0 | 0 | 0 | 0.00 |
| | 5 | 202 996 | 58 878 | 613 | 4156 | 3543 | 5.95 |
| | 10 | 206 948 | 57 892 | 3032 | 8107 | 5075 | 8.52 |
| | 15 | 210 717 | 56 741 | 5926 | 11 877 | 5950 | 9.99 |
| | 20 | 212 268 | 56 461 | 7176 | 13 428 | 6253 | 10.49 |
| | 25 | 215 648 | 54 948 | 9405 | 16 808 | 7403 | 12.43 |
| | 30 | 218 853 | 53 261 | 11 658 | 20 013 | 8354 | 14.02 |
| | 35 | 221 884 | 51 394 | 12 925 | 23 044 | 10 118 | 16.98 |
| | 40 | 224 744 | 49 342 | 14 916 | 25 903 | 10 988 | 18.44 |

phases, total *v/c* and saturation degree *x*. The multivariate regression method shown in Section 2.3 is also adopted here to distinguish whether the above factors pay significant impacts on the slope. A universal function between $P_q$ and CI is

$$\mathrm{CI}(P_q) = \alpha_3 P_q + b_3 \tag{12}$$

where $\alpha_3$ is the slope, and $b_3$ is the intercept.

In reality, $b_3$ equals 1.0. However, there are marginal differences between the intercepts in (11) and 1.0 because of fitting error. In this study, the differences are neglected and $b_3$ is set as 1.0.

Total ten groups of data are used in the regression and the output results are as follows

$$\left(e^{\alpha_3} = 5.946 - 2.664\log(\mathrm{CCL}) + 0.140 y_u - 0.049\lambda_c, \; . \; R^2 = 0.93\right) \tag{13}$$

$\alpha_3$ is affected by CCL, $y_u$ and $\lambda_c$. (13) can be written as

$$\alpha_3 = \ln\big(5.946 - 2.664\log(\mathrm{CCL}) + 0.140 y_u - 0.049\lambda_c\big) \tag{14}$$

In the above numerical experiments, the path flows of two directions are the same. However, in reality there may be difference between them. Other numerical experiments are also conducted and prove that $P_q$ in (14) can be calculated by the following equation

$$P_q = \frac{(P_{q1} + P_{q2})}{2} \tag{15}$$

where $P_{q1}$, $P_{q2}$ are proportion differences of current path flow out of maximum historical path flow of the two directions.

### 2.6 *Integrated correlation degree model of two adjacent intersections*

In Sections 2.3–2.5 the detailed relationships between contributing factors and CI are developed. To depict their joint impacts on CI, the following integrated correlation model is brought forward.

$$\begin{aligned}\mathrm{CI} &= 1 - \Big[(1 - \mathrm{CI}(C_D)) + (1 - \mathrm{CI}(L_c)) + (1 - \mathrm{CI}(P_q))\Big] \\ &= \mathrm{CI}(C_D) + \mathrm{CI}(L_c) + \mathrm{CI}(P_q) - 2\end{aligned} \tag{16}$$

where $\mathrm{CI}(C_D)$, $\mathrm{CI}(L_c)$ and $\mathrm{CI}(P_q)$ can be obtained by (4),

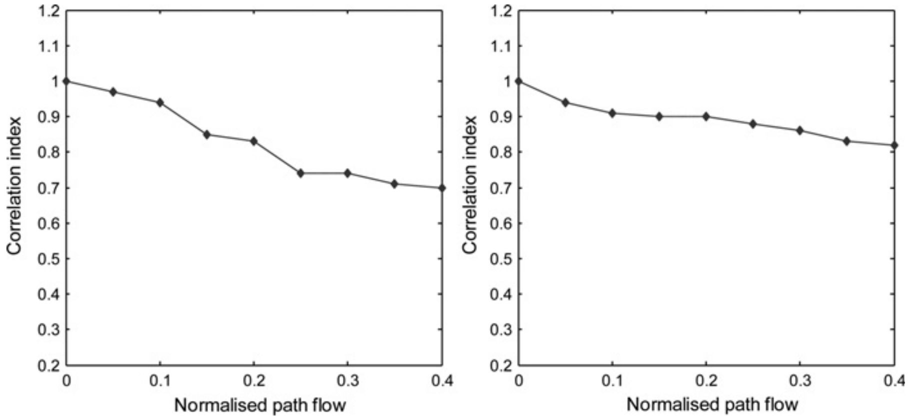


**Fig. 4** *Scatter diagrams between normalised path flow and CI*


doi: 10.1049/iet-its.2011.0224

(9), and (12), respectively. In (16), the term $1-\mathrm{CI}(C_{\mathrm{D}})$ indicates the decrease of correlation degree because of the cycle length difference between the two adjacent intersections. The terms in the square brackets indicate the total decrease of correlation degree because of the three contributing factors.

PI is the improved network performance when signal coordination is implemented. When PI is larger than 0, the coordinated mode can obtain better performance than isolated control mode. In such situation the two adjacent intersections can be partitioned into one subarea, otherwise they must be partitioned into different subareas. In this paper, CI is developed to simulate PI. When PI is larger than 0, CI is also larger than 0. Therefore 0 is set as the threshold value of CI to distinguish whether the two adjacent intersections can be partitioned into a same subarea.

## 3 Experiments and validation

An example is displayed to explain the correlation model established above. Field data are collected from two *T* type intersections in Fuzhou, the capital of Fujian Province, China. Sketches and phasing diagrams of the two intersections are shown in Fig. 5. The two intersections carry out three phases timing plans. Traffic volume of each lane is collected every 5 min and timing parameters are optimised and updated every 15 min.

To test whether CI can vary as the change of traffic state, two traffic scenarios are selected. One is based on the traffic flow operation from 10:45 to 11:00 on 6 December 2006. The other is based on the traffic flow operation from 16:45 to 17:00 on 6 December 2006. Traffic volumes of the two scenarios are shown in Table 4.

The differences between the two scenarios include two aspects. One is that the difference between cycle lengths of scenario 2 is larger than that of scenario 1. The other is that in afternoon more vehicles turn from Wuyi Road to Jintai Road and Fuxin Road, thus the path flow between the two coordinated phases is smaller than that of scenario 1. Table 5 shows the related parameters for the calculation of CI. From Table 5 we can find that the difference between the two cycle lengths increases from 10 to 17 s.

Then according to (16), the correlation degrees between A and B in the two scenarios are obtained and the results are shown in Table 6. In scenario 1 and 2, CI equals 0.59 and 0.13, respectively. Because two adjacent intersections can be partitioned into one subarea when CI is larger than 0, thus, in the two scenarios intersection A and B have the qualification to be combined. The CI in scenario 1 is larger than that in scenario 2. It is because of the larger differences between cycle lengths and smaller path flow between the two coordinated phases in scenario 2.

In scenario 1 CI is much larger than the threshold value 0. Whereas in scenario 2, CI is near to 0. This indicates that in scenario 1 signal coordination can obtain much better performance than isolated control schemes. And in scenario 2, though the performance of signal coordination is better than isolated control schemes, the advantage is not significant.

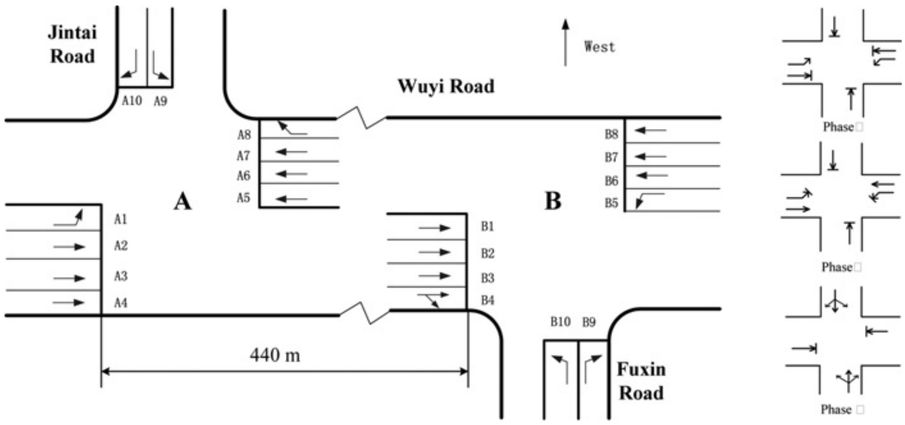


**Fig. 5** *Sketch and phasing diagram of the two adjacent intersections*

**Table 4** Arrival traffic volume of each lane

| Scenario 1 | | | | Scenario 2 | | | |
|---|---|---|---|---|---|---|---|
| Intersection A | | Intersection B | | Intersection A | | Intersection B | |
| Lane | Volume, pcu $h^{-1}$ | Lane | Volume, pcu $h^{-1}$ | Lane | Volume (pcu $h^{-1}$) | Lane | Volume pcu $h^{-1}$ |
| A1 | 268 | B1 | 544 | A1 | 355 | B1 | 512 |
| A2 | 616 | B2 | 592 | A2 | 572 | B2 | 512 |
| A3 | 608 | B3 | 560 | A3 | 584 | B3 | 504 |
| A4 | 626 | B4 | 372 | A4 | 572 | B4 | 452 |
| A5 | 516 | B5 | 308 | A5 | 440 | B5 | 376 |
| A6 | 524 | B6 | 442 | A6 | 448 | B6 | 442 |
| A7 | 508 | B7 | 468 | A7 | 420 | B7 | 468 |
| A8 | 308 | B8 | 452 | A8 | 388 | B8 | 444 |
| A9 | 276 | B9 | 304 | A9 | 284 | B9 | 312 |
| A10 | 356 | B10 | 272 | A10 | 336 | B10 | 300 |



*IET Intell. Transp. Syst.*, 2013, Vol. 7, Iss. 1, pp. 28–35
doi: 10.1049/iet-its.2011.0224

**Table 5** Parameters that related to the calculation of CI

| Scenario 1 | | | Scenario 2 | | |
|---|---|---|---|---|---|
| Parameters | Intersection A | Intersection B | Parameters | Intersection A | Intersection B |
| $C_c$, s | 85 | 75 | $C_c$,s | 91 | 74 |
| $\lambda_c$ | 0.45 | 0.43 | $\lambda_c$ | 0.41 | 0.375 |
| $x$ | 0.874 | 0.855 | $X$ | 0.89 | 0.85 |
| $Y$ | 0.78 | 0.75 | $Y$ | 0.796 | 0.75 |
| $Y_c$ | 0.39 | 0.37 | $Y_c$ | 0.365 | 0.32 |
| $Y_u$ | 0.39 | 0.38 | $Y_u$ | 0.43 | 0.43 |

**Table 6** Calculating results of CI for the two scenarios

| Parameters | $\alpha_1$ | $\alpha_2$ | $\alpha_3$ | CI ($C_D$) | CI ($L_c$) | CI ($P_q$) | CI |
|---|---|---|---|---|---|---|---|
| scenario 1 | − 1.77 | 1.865 | − 0.576 | 0.79 | 0.91 | 0.88 | 0.59 |
| scenario 2 | − 2.25 | 1.77 | − 0.73 | 0.58 | 0.87 | 0.68 | 0.13 |

**Table 7** Comparisons between signal coordination and isolated control in the two scenarios

| Scenario | 1 | 2 |
|---|---|---|
| performance of signal coordination/s | 79 692 | 81 326 |
| performance of isolated control/s | 64 128 | 76 638 |
| improved range | 19.5% | 5.66% |

To validate our conclusion, traffic data of the two scenarios are input into signal coordination algorithm and isolated control algorithm respectively. The control performances of signal coordination and isolated control of the two scenarios are produced, which are shown in Table 7.

From Table 7 we can find that in scenario 1, compared with isolated control, signal coordination can reduce total vehicle delay as much as 19.5%. However, in scenario 2 the proportion is only 5.66%, which indicates that there is not obvious difference between the control performances of signal coordination and isolated control. The results in Table 7 are accordance with that in Table 6.

Therefore we can conclude that the correlation degree model developed in this study can reflect the dynamic change of traffic state. Besides, CI is closely related to the change of PI, which indicates that CI can be an alternative for PI. Accordingly, CI is worth trusting in subarea partition.

Compared to the coordinatibility factor of Synchro, the calculation model of CI takes consideration into more contributing factors. Besides, determining the threshold value of CI is more reasonable. The experiences of engineers pay small impacts on CI. However, Synchro is widely used and accepted by the public. Our future research will develop statistic models for quantitatively assessing the generality of the correlation degree model.

## 4 Conclusions

This paper developed a correlation degree model between two adjacent intersections by taking consideration into three contributing factors, which are difference between cycle lengths, link length and path flow between upstream and downstream coordinated phases. A case study was displayed to explain the model and the results show that it is worth trusting in subarea partition.

This paper mainly focused on providing research thoughts for developing correlation degree model between two intersections. Future research will be focused on developing correlation degree model among multiple adjacent intersections and the subarea partition algorithm which can partition intersections with high-correlation degree into one subarea.

## 5 Acknowledgments

This study is supported by the National High Technology Research and Development Program of China (Grant No. 2011AA110304).We are grateful to Liang-Tay Lin and Shou-Min Tsao, their paper helps us find some usefully related literatures and provides us meaningful research thought.

## 6 References


1 Lin, L.T., Tsao, S.M.: 'A system approach on signal grouping for areawide control of computerized traffic system'. Proc. of 79th Annual Meeting of the Transportation Research Board, Washington, DC, USA, January 2000, pp. 1–21

2 Walinchus, R.J.: 'Real-time network decomposition and subnetwork interfacing', *Highw. Res. Rec.*, 1971, **366**, pp. 20–28

3 Yagoda, N.H.: 'Subdivision of signal systems into control areas', *Traffic Eng.*, 1973, **43**, (12), pp. 42–45

4 Chang, E.C.P.: 'Evaluation of interconnected arterial traffic signals', *Transp. Plan. J. Q.*, 1986, **1**, (15), pp. 137–156

5 Bie, Y.M., Wang, D.H., Wei, Q., *et al*: 'Development of correlation degree model between adjacent signal intersections for subarea partition'. Proc. of the 11th Int. Conf. of Chinese Transportation Professionals, Nanjing, China, August 2011, pp. 1–11

6 Lin, L.T., Huang, H.J.: 'A linear model for determining coordination of two adjacent signalized intersections', *J. Modeling Manage.*, 2009, **4**, (2), pp. 162–173

7 Husch, D., Albeck, J.: 'Synchro 6: traffic signal software; user guide' (Calif, Albany, 2003)

8 Tian, Z., Urbanik, T.: 'System partition technique to improve signal coordination and traffic progression', *J. Transp. Eng.*, 2007, **133**, (2), pp. 119–128

9 Robertson, D.I.: 'Optimizing networks of traffic signals in real time-the SCOOT method', *IEEE Trans. Veh. Technol.*, 1991, **40**, (1), pp. 11–15

10 Sims, A.G., Dobinson, K.W.: 'The Sydney coordinated adaptive traffic (SCAT) system philosophy and benefits', *IEEE Trans. Veh. Technol.*, 1980, **29**, (2), pp. 130–137

11 Mirchandani, P., Head, L.: 'RHODES: A real-time traffic signal control system: architecture, algorithms, and analysis', *Transp. Res. Part C*, 2001, **9**, (6), pp. 415–132

12 Robertson, D.I.: 'TRANSYT A traffic network study tool-Report'. *No. 253*, TRRL Laboratory, London, UK, 1969

13 Transportation Research Board: 'Highway Capacity Manual'. Transportation Research Board, 2000